A98-31456

ICAS-98-1,4,2

EFFECT OF LEX SURFACES ON LATERAL-DIRECTIONAL DYNAMIC STABILITY OF COMBAT AIRCRAFT

Lars E. Ericsson
Mountain View, California 94040
and
Martin E. Beyers
Institute for Aerospace Research
Ottawa, Ontario, K1A OR6 Canada

Abstract

The role of configurational effects and associated maneuver-dependent departure characteristics in placing limitations on high-alpha maneuvers has been examined. The unsteady aerodynamics of advanced aircraft are considered with reference to two radical maneuvers, the Herbst and cobra maneuvers, for which the initial pitch-up phases are very similar but the high-alpha maneuvering phases are distinctly different. To successfully perform air combat maneuvers the aircraft must display adequate lateral-directional dynamic stability over the complete alpha range of the maneuver.

Nomenclature

b	wing span
d	maximum body diameter
n	yawing moment, coefficient $C_n = n/q_\infty Sb$
N	normal force, coefficient $C_N = N/ q_\infty S$
q_∞	dynamic pressure, $= \rho_\infty U_\infty^2/2$
r	yaw rate
Re	Reynolds number, $Re = U_\infty d /\nu_\infty$
S	reference area, $\pi d^2/4$ or projected wing area
t	time
U_∞	freestream velocity
V	circumferential crossflow velocity
x	axial distance from apex
Y	side force, coefficient $C_Y = Y/q_\infty S$
α	angle of attack
$\dot{\bar{\alpha}}$	pitch-rate-induced angle at the nose tip, $= x_{CG}\, \dot{\alpha} /U_\infty$
β	angle of sideslip
θ_A	forebody apex half-angle
ν	kinematic viscosity
ρ	air density
φ	body azimuth
ϕ	body-fixed roll angle
ψ	coning angle
Ω	dimensionless coning rate, $= \dot{\psi}\, b/2U_\infty$

Subscripts

CG	center of gravity (rotation center)
I	initial
∞	freestream conditions

Derivative Symbols

$\dot{\psi} = \partial\psi/\partial t$; $C_{nr} = \partial C_n/\partial(rb/2U_\infty)$; $C_{n\dot{\beta}} = \partial C_n/\partial(\dot{\beta}\, b/2U_\infty)$

Introduction

In response to the increased demands during the 1980s for high maneuverability radical "supermaneuver" concepts were introduced,[1] which subsequently became something of a test of potency for contemporary high-performance aircraft. It soon became clear that not every aircraft could perform these maneuvers. In comparing the aircraft that are known to have made the grade, some common configurational characteristics emerge. Thus, the full-scale flight experience provides valuable information, which can serve as a basis for conceptual analyses[2-4] of the dynamic stability of these aircraft under maneuvering flight conditions. In the Herbst supermaneuver[1,2] the pitch-up motion ends with a sharp lateral turn, a so-called velocity vector roll (Fig. 1), whereas the

cobra maneuver is a pure pitching motion,[3] terminated by a pitch-down from $\alpha \approx 120°$.

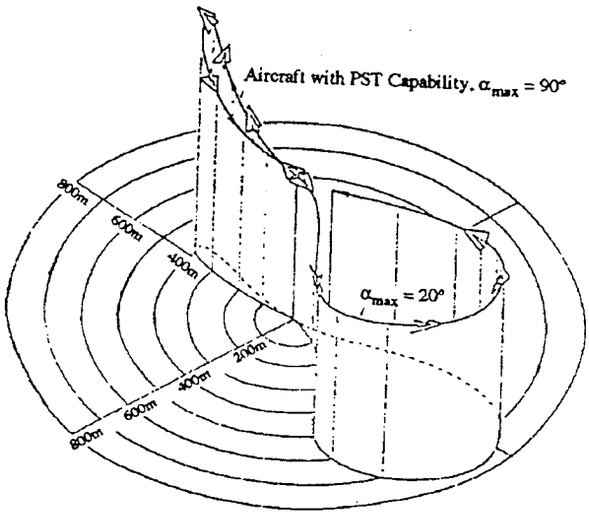

Fig. 1. Herbst supermaneuver.[1]

The unsteady aerodynamics are very sensitive to forebody configurational characteristics and, in particular, to where leading-edge extension (LEX) and wing surfaces are located relative to the base of the slender forebody; e.g. well aft and/or outboard of the air intakes, as in the case of the F-14 aircraft[5] (Fig. 2), or extending to the base of the forebody, as in the case of the F-16 aircraft[6] (Fig. 3). Whereas LEX surfaces were originally incorporated in the aircraft design to improve post-stall lift characteristics they have been shown to have also a very beneficial effect on the dynamic lateral stability.[7]

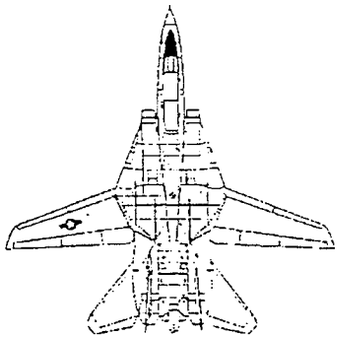

Fig. 2. F-14 Tomcat.[5]

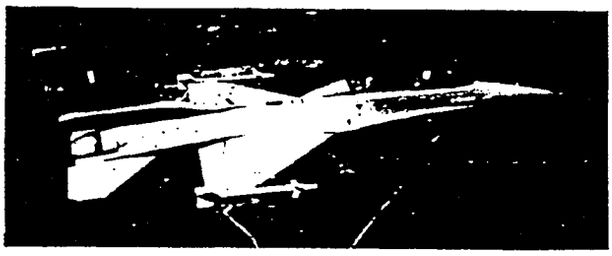

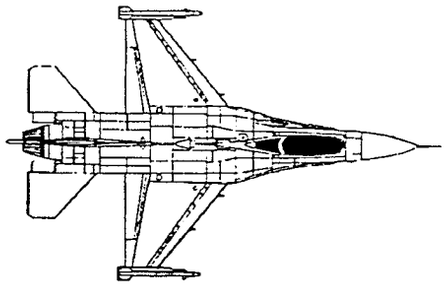

Fig. 3. F-16 Fighting Falcon.[6]

Background

Test results for an advanced aircraft configuration with the F-14 type of forebody geometry[8] (Fig. 4) showed that the high-alpha dynamic instability in yaw was generated by the loads on the slender forebody. Consequently,

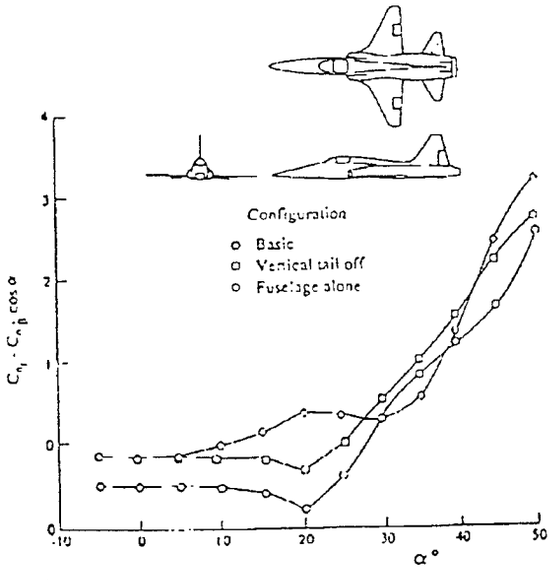

Fig. 4. Yaw damping characteristics of an advanced aircraft model.[8]

body-alone aerodynamics are representative of the high-alpha characteristics of the complete aircraft, and the flow visualization results for an l/d = 10.3 blunted cone-cylinder body in pitch-up or pitch-down motions[9,10] are of interest. They showed that asymmetric forebody flow separation, causing the dynamic yaw instability in Fig. 4, developed even at pitch rates well above those reached in the cobra maneuvers[11] (Fig. 5). Thus, the dynamic instability in yaw, developed at zero pitch rate[8] (Fig. 4), is likely to exist also at the high pitch rates of the Herbst and cobra maneuvers. As the moving wall effects are largely concentrated in the boundary layer build-up region near the flow stagnation point, Magnus lift results for a rotating circular cylinder[12] are indicative of the moving wall effects for the translating circular cross-section of a slender forebody[13] at moderately high angles of attack, $\alpha < 60°$. Using this assumption[14] provided satisfactory prediction of the experimental results for a coning cone-cylinder[15] (Fig. 6).

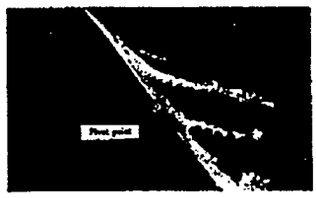

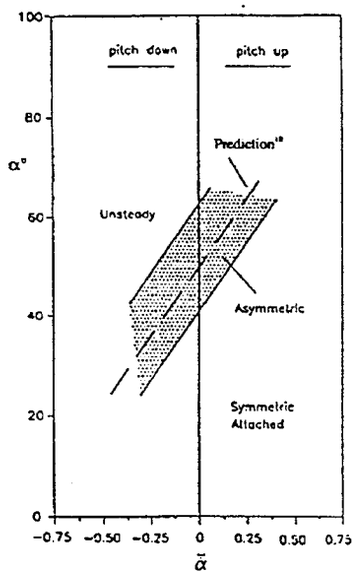

Fig. 5. Effect of pitch rate $\bar{\dot{\alpha}}$ on alpha region for asymmetric crossflow separation on a 10.3 caliber cone-cylinder.[9]

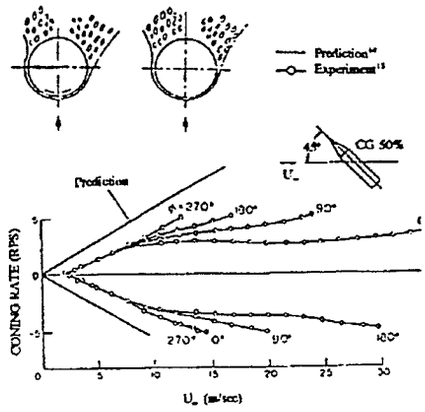

Fig. 6. Free-to-spin coning rate of cone-cylinder.

Analysis

Thus, the moving wall effect[13] on the forebody flow separation will significantly amplify the control-induced yawing moment. In addition, a sudden increase of the pitch-up moment will be generated by the change to an asymmetric crossflow separation geometry. Recent tests[16] showed that removing the nose strakes on an advanced aircraft model (Fig. 7), thereby allowing the development of static, asymmetric crossflow separation, more than doubled the nose-up pitching moment (Fig. 8).

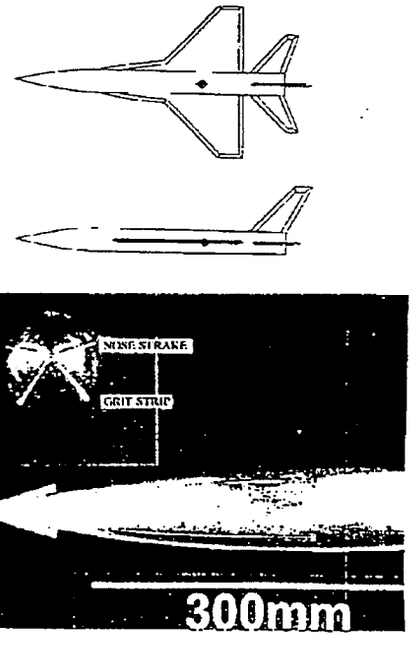

Fig. 7. AGARD WG16 generic combat aircraft model.[16]

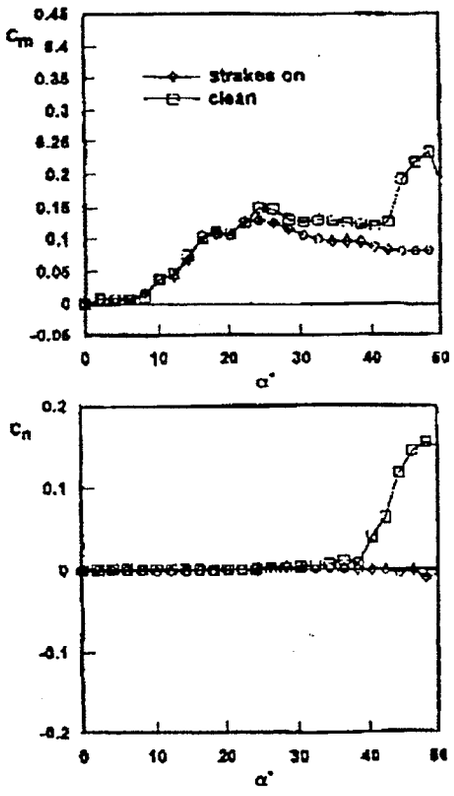

Fig. 8. Effect of nose strakes on $C_m(\alpha)$ and $C_N(\alpha)$ of AGARD WG16 aircraft model.[16]

Thus, a strong pitch-up tendency is associated with the crossflow separation asymmetry established during a rapid roll around the velocity vector. This could have provided the conditions for a stable spin mode of the F-14 aircraft at very high angles of attack.[17] Rotary-rig tests of the AGARD WG16 generic model of a combat aircraft[18] (Fig. 7) produced the results shown in Fig. 9. Instead of the high-alpha pro-coning C_n, expected at subcritical flow for forebody-dominated characteristics[7] (Fig. 4), the data[18] in Fig. 9 for the clean forebody show an anti-coning trend. When looking for the cause of this difference one notices one obvious difference between the tested aircraft models, i. e. the presence of LEX surfaces only on the AGARD model in Fig. 7. It is discussed in Ref. 7 how the LEX-induced upwash could have caused this difference. In the rotary-rig tests[7,16,18,19] the effect of the LEX-induced upwash is influenced by the coning motion as illustrated in Fig. 10. The coning generates a local sideslip that decreases the effective leading-edge sweep of the LEX on the windward, advancing side and increases it on the opposite, receding side.

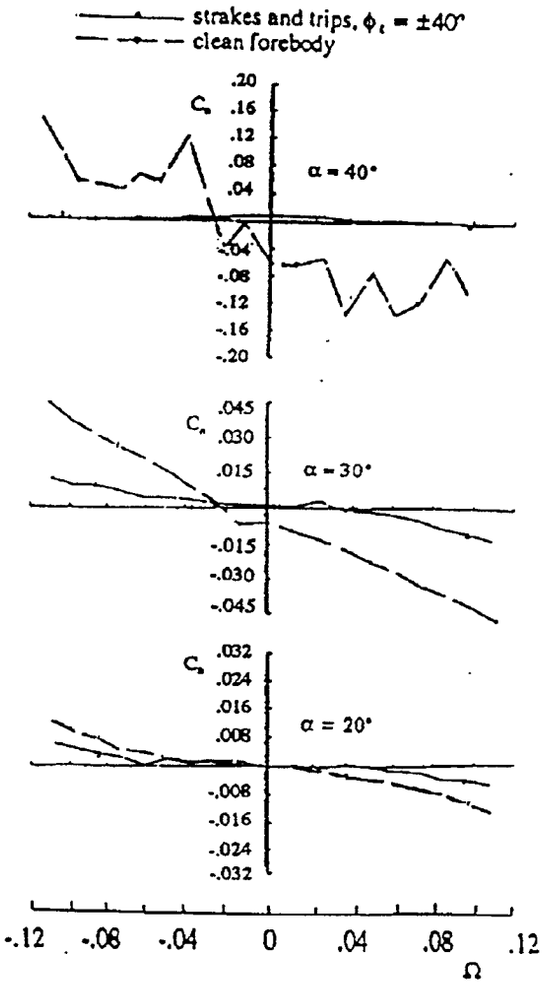

Fig. 9. Effect of nose strakes on $C_n(\Omega)$ for α = 20, 30, and 40 deg.[18]

This results in a stronger LEX-induced upwash on the advancing side than on the receding side. As a consequence of the dominance of the LEX-induced upwash, the crossflow separation and associated vortex shedding on the slender forebody is affected as illustrated in the sketches in Fig. 10. That is, instead of generating a pro-coning force as in the case of no LEX surfaces (Fig. 10a), the LEX-induced upwash causes the crossflow separation to generate an anti-coning force on the forebody (Fig. 10b), in agreement with the high-alpha data trend in Fig. 9. That the LEX surfaces act as shown in Fig. 10, providing an anti-coning moment contribution rather than simply being delaying the

occurrence of asymmetric crossflow separation on the forebody is demonstrated by the experimental

results in Fig. 9, where the nose strakes delay the asymmetric crossflow separation to $\alpha > 40°$.

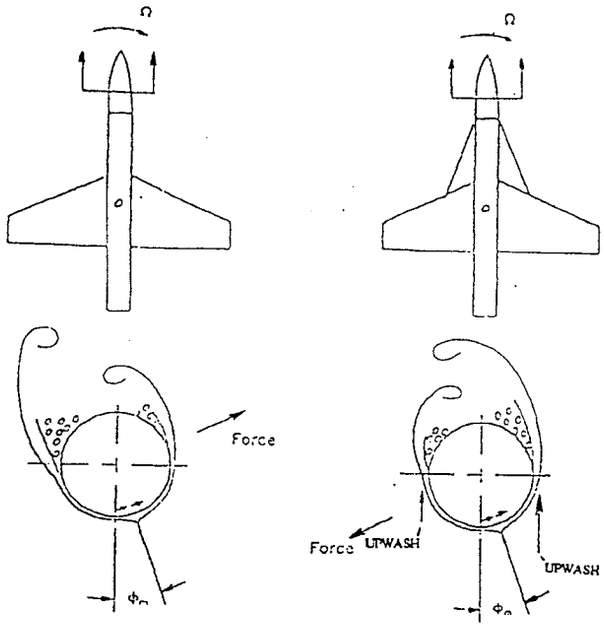

a. Without LEX b. With LEX

Fig. 10. Crossflow separation on coning slender forebody.[7]

In view of the above discussion of the effect of LEX surfaces it is interesting to note that in the documented cases of aircraft known to have performed the cobra maneuver,[20,21] the Su-27 (Ref. 22 and Fig. 11a) and the MiG-29 (Ref. 23 and Fig. 11b), the aircraft have LEX surfaces that extend to the base of the slender forebody. In addition, asymmetric forebody crossflow separation may have been delayed somewhat by the presence of a nose boom.[24]

The difficulty in performing the Herbst supermaneuver with a slender-nosed aircraft was overcome by using thrust vectoring on the X-31 aircraft. Test pilot Karl Lang performed the supermaneuver, using a turning radius of 475 ft compared to the 2700 ft radius of a coordinated, steady turn.[25] To decouple lateral and longitudinal control mechanisms, as was accomplished here by using thrust vectoring for lateral control and all movable canards for pitch control, appears to be important in order to minimize the tendency towards adverse control/vehicle dynamics coupling.[26] Moreover, for symmetric deflection

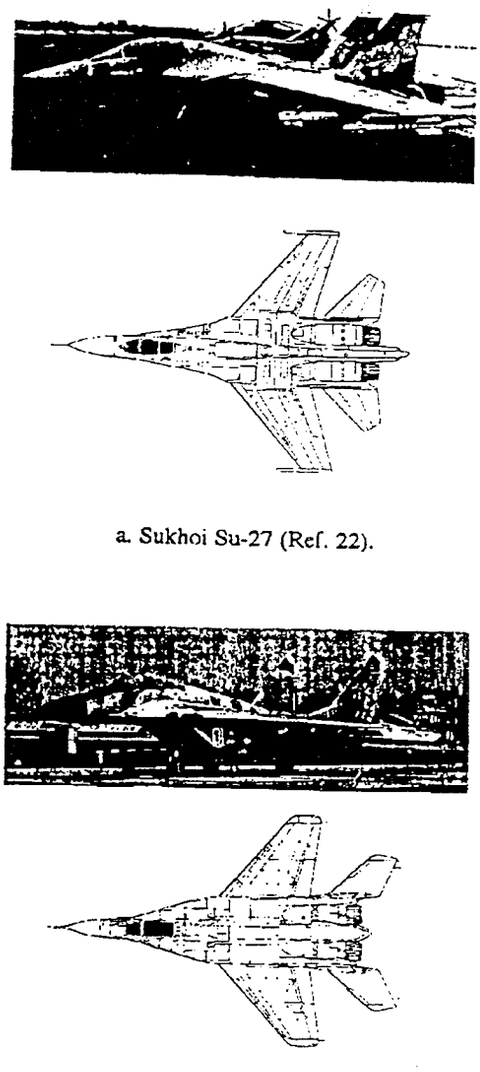

a. Sukhoi Su-27 (Ref. 22).

b. Mikoyan MiG-29M (Ref. 23).

Fig. 11. Aircraft known to have performed the cobra maneuver.

the canards with swept leeding edges will act as the LEX surfaces (Fig. 10), generating an anti-spin force on the forebody in the presence of a coning motion.

Slender Forebody Aerodynamics

The complicated nature of the loads induced on a slender forebody in pitch oscillations[10] are well illustrated by the C_n results in Fig. 12, obtained on the AGARD WG16 generic combat aircraft model with nose strakes and boundary layer grit strips[16] (Fig. 7). They are unusual in

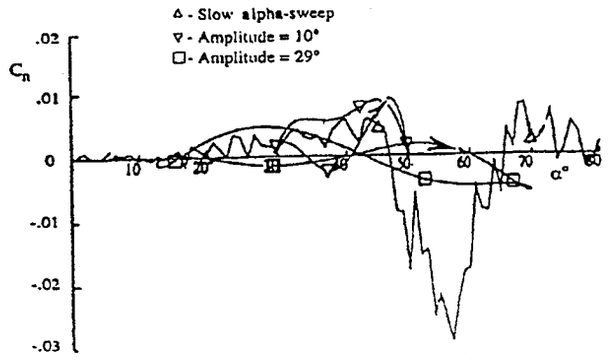

Fig. 12. Effect of large-amplitude oscillatrions in pitch on $C_n(\alpha)$ of AGARD WG16 model with nose strakes and boundary layer trips.[16]

two respects. First, a static yawing moment , $|C_n| > 0$, is measured at $\beta = 0$ for $\alpha > 45°$ even though the strakes force the flow separation to be symmetric at the nose tip.[24] The nose strakes only delay the occurrence of the separation asymmetry, from $\alpha > 30°$ to $\alpha \geq 45°$. This is in agreement with experimental results for the X-31 aircraft,[27] indicating that a limited range exists at high alpha in which steady asymmetric crossflow separation can develop aft of the nose region affected by the strakes. Surface flow visualization results at $\alpha = 46°$ for the AGARD WG16 model with a clean forebody[28] suggest that a new vortex pair is being generated two calibers downstream of the nose tip. This is in basic agreement with existing experimental evidence.[24] If the forebody is long enough the presence of the symmetric first vortex pair produced by the nose strakes can only delay, not prevent, the occurrence of asymmetric flow separation farther downstream. The location where the second vortex pair starts on the clean forebody of the WG16 model is approximately one strake length behind the trailing edges of the nose strakes.[28]

It is more challenging to explain the other result in Fig. 12, i.e. the capability of a very modest pitch rate to eliminate the asymmetric crossflow separation existing at $45° < \alpha < 65°$ for essentially static flow conditions (Slow alpha-sweep). As the dynamic $C_n(\alpha)$ loops above and below $\alpha = 40°$ are quite similar, there cannot be any significant effect of forebody flow asymmetry at $\alpha > 40°$. Experimental results for an ogive-cylinder[29,30] (Fig. 13) show that the modest pitch-up rate $\dot{\alpha}\, d/U_\infty = 0.0027$ significantly changed the crossflow separation characteristics from those existing at $\dot{\alpha} = 0$. The crossflow acceleration

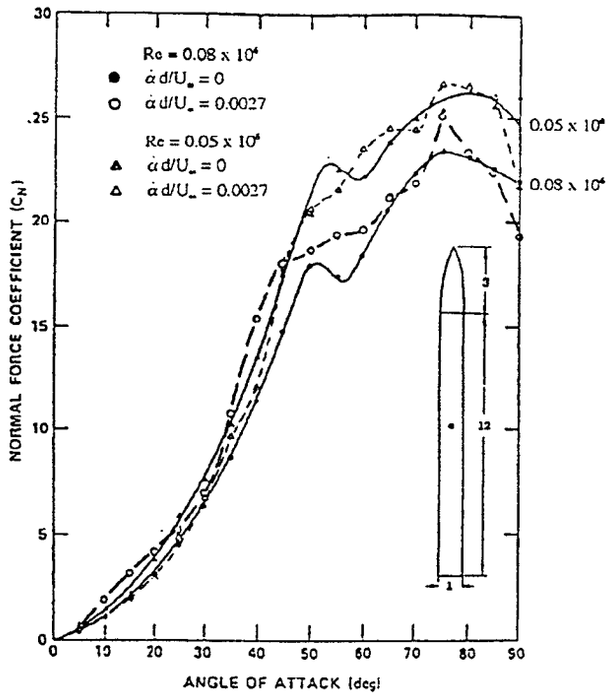

Fig. 13. Pitch rate effect on ogive-cylinder normal force at critical flow conditions.[29]

generated by the pitch-up motion apparently had an effect similar to that of nose strakes[31] (Fig. 14), preventing the asymmetric flow separation with associated side force and increased normal force from developing. The crossflow separation process can be simulated using the impulsively started cylinder flow analogy.[32,33] In that case the circumferential crossflow velocity V is a function $V = f(V_I)$ of the initial velocity $V_I = U_\infty \sin \alpha$, and the crossflow acceleration can be written

$$dV/dt = (\partial f/\partial V_I)\, U_\infty \cos \alpha\ \dot{\alpha} \qquad (1)$$

Equation (1) shows that the crossflow acceleration is largest at $\alpha = 0$ and becomes zero at $\alpha = 90°$.

This is in agreement with the data trend in Fig. 13, where the difference from the static normal force

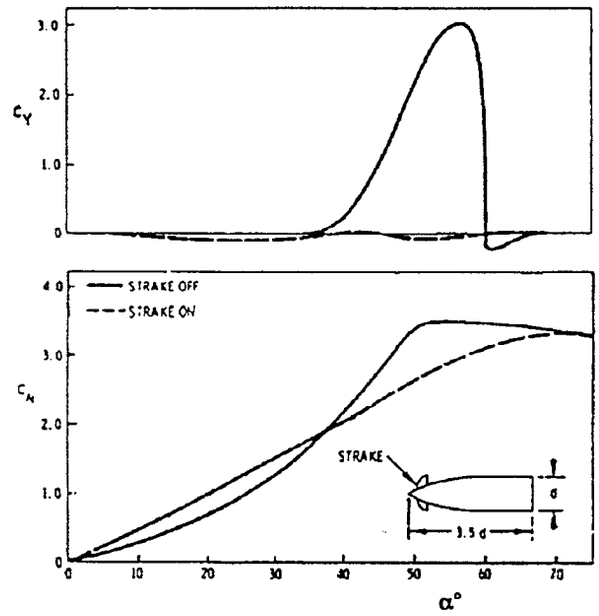

Fig. 14. Effect of nose strakes on the $C_Y(\alpha)$ and $C_N(\alpha)$ characteristics of a pointed ogive-cylinder.[31]

is largest at low angles of attack, and becomes negligible at $\alpha > 60°$, where the increased data scatter is the likely result of Karman type flow instability.[24] The kink at $\alpha > 40°$ in the static $C_N(\alpha)$ curves is the result of the lift-off of one member of the asymmetric vortex pair, allowing the other, lower vortex to move inboard, thereby generating more normal force. This data trend is clearly exhibited by the experimental results[31] in Fig. 14. The cylindrical afterbody in Fig. 13, not present in Fig. 14, provided an additional C_N increase at higher angles of attack.

One question that needs to be answered is why the accelerated flow effect is so much larger at Re = 0.08 x 10^6 than at Re = 0.05 x 10^6. The quoted[29] 6 % decrease of the freestream speed when the model was pitched from $\alpha = 0$ to $\alpha = 90°$ indicates that the model blockage was substantial, suggesting that the associated increased turbulence level could have been responsible for the early establishment of critical crossflow conditions.[34] With that scenario the experimental results in Fig. 13 suggest that at Re = 0.08 x 10^6 the static characteristics were obtained at critical flow conditions, whereas at Re = 0.05 x 10^6 laminar flow conditions existed. This is consistent with the fact that the decreased crossflow drag at $\alpha = 90°$ resulted in 10% lower C_N at Re = 0.08 x 10^6 than at Re = 0.05 x 10^6. Furthermore, at Re = 0.08 x 10^6 it appears that the accelerated flow effects during the pitch-up were powerful enough to produce laminar flow conditions, generating C_N values equal to or larger than the static values for Re = 0.05 x 10^6 at $\alpha < 50°$. That the crossflow conditions on the clean forebody in the test at Re = 0.2 x 10^6 of the AGARD WG16 model (Fig. 7) were close to the critical range could be verified by a comparison with the force data at Re = 0.15 and 0.30 x 10^6 (Ref. 28). The presence of the trips at $\varphi = \pm 40°$ on the forebody (Fig. 7b) could therefore have played a significant role in establishing critical crossflow conditions at Re = 0.2 x 10^6.

Another question that needs to be answered is why the predicted[10] $\dot{\alpha}$ dependence of the α boundaries for asymmetric crossflow separation agrees so well with the experimental data trend[9] (Fig. 5), despite the fact that no consideration was given to the accelerated flow effect discussed here, Eq. (1). The likely reason is the large difference in the magnitudes of the pitch rates. It has been shown that the roll-rate-induced camber effect for a 65 deg delta-wing-body configuration is saturated at a very modest roll rate, whereas the convective time lag effects continue to grow unabatedly to very high roll rates.[35,36] A similar rate saturation phenomenon has been observed for the pitch-rate-induced camber effect on the vortex characteristics of a 45 deg delta wing.[37,38] The pitch rate $\bar{\dot{\alpha}} = \dot{\alpha} d/U_\infty = 0.0027$ in Fig. 13 gives $\bar{\dot{\alpha}} = \dot{\alpha} x_{CG}/U_\infty = 0.022$, well below any rate saturation value in Fig. 5. That is, in Fig. 5 the convective time lag is the dominant effect, whereas in Fig. 13 the accelerated flow effect dominates.

Maneuver Time History

The question which has to be answered in order to assess the lateral-directional control

requirements in the supermaneuver is whether or not asymmetric flow separation conditions will be established over some part of the alpha range. Considerations of the flight conditions should in themselves give an indication of the likelihood of departure.

The entry into the Herbst post-stall maneuver occurs at high subsonic Mach numbers, where the crossflow separations are predominantly of the supercritical type. At moderate altitudes the flow conditions are likely to remain supercritical during the deceleration period when the angle of attack climbs into the range for asymmetric crossflow separation. Since the coning motion is initiated before that point, there is a possibility of departure into a steep spin when the pitching moment changes sign at high alpha. With further deceleration as alpha approaches 90°, the critical/supercritical crossflow separation can be established over part of the forebody, facilitating the departure into flat spin. Thus, for forebody-dominated aircraft configurations the danger of departure would be present at more than one segment of the Herbst maneuver. Consequently, even if the aircraft manages to traverse uneventfully the α range for asymmetric crossflow separation, the control-induced lateral motion can lead to flat spin when the critical/supercritical flow asymmetry occurs in the range $70° < \alpha < 90°$. The commanded maximum yaw rate of the F-14 aircraft,[4] 180 deg/sec, would result in lateral velocities at the nose tip that could generate a flat-spin-driving moment.[2]

Even in the absence of a control-induced input the forebody flow is likely to become asymmetric at $\alpha > 2\ \theta_A$. Because of the flow field time lag the crossflow asymmetry could persist to angles of attack approaching 90 deg. Thus, departure into flat spin is possible. This tendency will be independent of the presence of nose strakes, as at these high incidences asymmetric crossflow separation will develop on the forebody aft of the strakes.[7] This behavior is consistent with observations for the X-31 at $\alpha \geq 60°$ (Ref. 27) as well as for the AGARD WG16 model (Fig. 7) at $\alpha \geq 45°$ (Refs. 16 and 28). Maneuver control through forebody blowing[2,24,39] will be ineffective at these high angles of attack.

In contrast to the Herbst supermaneuver, where a large control-induced yaw rate will be generated, favoring departure into flat spin, in the case of the cobra maneuver, performing a pitch-up to $\alpha = 70°$, the steep spin that might result at the equilibrium conditions will occur at a lower rotation rate and possibly higher angle of attack because of the reduced pitch-down moment in the presence of asymmetric crossflow separation (Figs. 8 and 14). On the other hand, if the aircraft is pitched up towards $\alpha = 90°$, the full negative pitching moment generated by the tail surfaces has to be balanced, which could lead to a fast flat spin that may not be recoverable. The conditions for spin equilibrium also require a balance of lateral forces, which is provided at finite sideslip.

The conditions associated with fluid/motion coupling at lower altitudes are dangerous to cover in flight tests and difficult to investigate in wind tunnels because of the high Reynolds numbers that have to be simulated.[40] As a result, very little data is available for these flow conditions. Consequently, more analysis is needed of fluid/motion coupling at high subsonic Mach numbers and high Reynolds numbers. Until such data become available the documented flight experience of the Su-27 and MiG-29 will provide the sole corroboration of supermaneuver predictions.

Conclusions

An analysis of the unsteady aerodynamics of combat aircraft, performing the Herbst and cobra maneuvers, has shown that a dominant source of the highly nonlinear vehicle dynamics at high angles of attack is the effect of the asymmetric crossflow separation occurring on a slender forebody. A study of the rotary-rig test results for the subscale AGARD WG16 combat aircraft model demonstrates that the highly nonlinear effect on the unsteady aerodynamics of angular rate and oscillation amplitude can be explained by applying the information obtained in one-degree-of-freedom dynamic tests with subscale models of missiles and aircraft geometries. While the test results analyzed are not representative of full-scale flight conditions, largely because of the habitual use of boundary layer trips, the methodology used in the present analysis is fully applicable to the (more straightforward) analysis of the unsteady aerodynamics existing at full-scale Reynolds numbers. The analysis demonstrates that the presence of wing LEX surfaces on the aircraft

performing these radical maneuvers could have provided the needed dynamic lateral stability.

References

1. Herbst, W. B., "Dynamics of Air Combat," Journal of Aircraft, Vol. 20, No. 7, 1983, pp. 594-598.

2. Ericsson, L. E. and Beyers, M. E., "Conceptual Fluid/Motion Coupling in the Herbst Supermaneuver," Journal of Aircraft, Vol. 34, No. 3, 1997, pp. 271-277.

3. Ericsson, L. E., "Cobra Maneuver Considerations," ICAS-92-4.6.5, Sept. 1994.

4. Beyers, M. E. and Ericsson, L. E., "Unsteady Aerodynamics of Combat Aircraft Maneuvers," AIAA Paper 97-3647, Aug. 1997.

5. Goodman, R. J. and Conigliaro, P. E., "F-14A Low Altitude High Angle of Attack Simulation and Flight Test Program," AIAA Paper 86-9774, April 1986.

6. Jane's All the World's Aircraft, 1989-1990, John W. R. Taylor editor, p. 412.

7. Ericsson, L. E. and Beyers, M. E., "Wind Tunnel Aerodynamics in Rotary Tests of Combat Aircraft Models," AIAA Paper 97-0729, Jan. 1997. (Accepted for publication in J. Aircraft).

8. Grafton, S. B., Chambers, J. R., and Coe, Jr., P. L., "Wind-Tunnel Free-Flight Investigation of a Model of a Spin Resistant Fighter Configuration," NASA TN D-7716, June 1974.

9. Montevidas, R. E., Reisenthel, P., and Nagib, H. N., "The Scaling and Control of Vortex Geometry Behind Pitching Cylinders," AIAA Paper 89-1003, June 1989.

10. Ericsson, L. E., "Unsteady Flow Separation on Slender Bodies at High Angles of Attack," Journal of Spacecraft and Rockets, Vol. 30, No. 6, 1993, pp. 689-693.

11. Skow, A. M., "An Analysis of the SU-27 Flight Demonstration in the 1989 Paris Air Show," Society of Automotive Engineers TP 901001, April 1990.

12. Swanson, W. M., "The Magnus Effect: A Summary of Investigations to Date," Journal of Basic Engineering, Vol. 83, Sept. 1961, pp. 461-470.

13. Ericsson, L. E., "Moving Wall Effects in Unsteady Flow," Journal of Aircraft, Vol. 25, No. 11, 1988, pp. 977-990.

14. Ericsson, L. E., "Prediction of Slender Body Coning Characteristics," Journal of Spacecraft and Rockets, Vol. 28, No. 1, 1991, pp. 43-49.

15. Yoshinaga, T., Tate, A., and Inoue, K., "Coning Motion of Slender Bodies at High Angles of Attack in Low Speed Flow," AIAA Paper 81-1899, Aug. 1981.

16. Cooperative Programme on Dynamic Wind Tunnel Experiments for Maneuvering Aircraft, Report of AGARD FDP WG16, AGARD-AR-305, Ch. 5, October 1996.

17. Jahnke, C. C. and Culick, F. E. C., "Aplication of Bifurcation Theory to the High-Angle-of -Attack Dynamics of the F-14," Journal of Aircraft, Vol. 31, No. 1, 1994, pp. 26-34.

18. Tristrant, D. R., Gauthier, F. F., and Vanmansart, M. G., "Dynamic Tests in ONERA-IMFL Lille Wind Tunnel with AGARD Generic Fighter Model," Preliminary Report, IMFL 94113, Nov. 1994.

19. Beyers, M. E. and Ericsson, L. E., "Extraction of Subscale Free-Flight Aerodynamics from Rotary Tests of Combat Aircraft," AIAA Paper 97-0730, Jan. 1997.

20. Aviation Week, Sept. 1990, p. 32.

21. Aviation Week, July 1990, p. 29.

22. Jane's All the World's Aircraft, 1992-1993, Mark Lambert editor, p. 243.

23. Jane's All the World's Aircraft, 1995-1996, Paul Jackson editor, p. 342.

24Ericsson, L. E. and Reding, J. P., "Asymmetric Flow Separation and Vortex Shedding on Bodies of Revolution," Chapter 10, Tactical Missile Aerodynamics, General Topics, Vol. 141, Progress Astro. and Aero. Series, 1992, pp. 391-452.

25. Brown, S. F., "It Went Thataway," Popular Science, Oct. 1993, p. 26.

26. Huber, P. and Galleithner, H., "X-31A High Angle of Attack and Initial Post Stall Flight Testing," Paper 11, AGARD CP-519, May 1992.

27. Alcorn, C. W., Croom, M. A., and Francis, M. S., "The X-31 Experiment: Aerodynamic Impediments to Post-Stall Agility," AIAA Paper 95-0362, Jan. 1995.

28. Cai, H. J. and Beyers, M. E., "Oscillatory Experiments on the AGARD WG16 CA Model," National Research Council Canada, IAR-AN-83, Sept. 1995.

29. Smith, L. H., "Aerodynamic Characteristics of an Axisymmetric Body Undergoing a Uniform Pitching Motion," Ph. D. Thesis, Naval Postgraduate School, Monterey, California, Dec. 1974.

30. Smith, L. H. and Nunn, R. H., "Aerodynamic Characteristics of an Axisymmetric Body Undergoing a Uniform Pitching Motion," Journal of Spacecraft and Rockets, Vol. 13, No. 1, Jan. 1976, pp. 8-14.

31. Coe, P. L., Chambers, J. R., and Letko, W., "Asymmetric Lateral-Directional Characteristics of Pointed Bodies of Revolution at High Angles of Attack," NASA TND-7095, Nov. 1972.

32. Allen, H. J. and Perkins, E. W., "Characteristics of Flow Over Inclined Bodies of Revolution,"NACA RM-A50L07, March 1951.

33. Sarpkaya, T., "Separated Flow About Lifting Bodies and Impulsive Flow About Cylinders," AIAA Journal, Vol. 4, No. 3, 1966, pp. 414-426.

34. Ericsson, L. E. and Beyers, M. E., "Nonlinear Rate and Amplitude Effects on a Generic Combat Aircraft Model," AIAA Paper 98-0409. Jan. 1998.

35. Grismer, D. S. and Jenkins, J. E., "Critical-State Transients for a Rolling 65° Delta Wing," AIAA Paper 96-2432, June 1996.

36. Ericsson, L. E., "Time History Effects on a Rolling 65 Deg Delta-Wing-Body Configuration," AIAA Paper 97-3645, Aug. 1997.

37. Cipollo, K. M. and Rockwell, D., "Flow Studies on Stalled Delta Wing Subjected to Small Amplitude Pitching Oscillations," AIAA Journal, Vol. 33, No. 7, 1995, pp. 1256-1262.

38. Ericsson, L. E., "Partial-Span Leading-Edge Vortex Characteristics in High Rate Oscillations in Pitch," Journal of Aircraft, Vol. 34, No. 3, 1997, pp. 443-445.

39. Ericsson, L. E., "Control of Forebody Flow Asymmetry- A Critical Review," AIAA Paper 90-2833, Aug. 1990.

40. Ericsson, L. E., "Effects of Transition on Wind Tunnel Simulation of Vehicle Dynamics," Prog. Aerospace Sci., Vol. 27, 1990, pp. 121-144.